IN SITU STUDIES OF THE VIBRATIONAL AND ELECTRONIC PROPERTIES OF Si NANOPARTICLES

J. R. FOX*, I. A. AKIMOV*, X. X. XI*, AND A. A. SIRENKO*
* Department of Physics, Penn State University, University Park, Pennsylvania 16802

ABSTRACT

We report on *in situ* studies of the vibrational properties of ultra-thin Si layers grown by dc magnetron sputtering in ultrahigh vacuum on amorphous MgO and Ag buffer layers. The average thickness of the Si layers ranged from monolayer coverage up to 200 Å. The interference enhanced Raman scattering technique has been used to study changes in the phonon spectra of Si nanoparticles during the crystallization process. Marked size-dependencies in the phonon density of states of the Si quantum dots and the relaxation of the **k**-vector conservation condition with decrease in size of the Si nanoparticles have been detected. Electron energy loss spectra have been collected for amorphous and crystallized Si nanoparticles on SiO_2 buffer layers and the difference in the onset of the electronic transitions have been found.

INTRODUCTION

As the size of condensed matter systems is reduced in one or more dimensions to nanoscale levels, the electron and phonon states are influenced by confinement and surface effects. The discovery of visible luminescence at room temperature from porous Si increased interest in the modification of silicon's electronic and vibrational properties with size [1,2]. Nanometer-sized Si-based structures prepared by a wide variety of methods have been intensively investigated [2-5]. Recent experimental studies, focused on the modification of the electronic states of nanocrystalline Si (nc-Si), report substantial changes in the luminescence properties and optical gap which are attributed to quantum confinement of the electronic states and a breakdown of **k**-vector conservation [6-8].

Theoretical [9,10] and experimental [11] studies of semiconductor nanocrystallites (or quantum dots) demonstrate the modification of the phonon spectra due to the confinement of the optical and acoustic vibrations. With decreasing particle size, Raman spectra change due to relaxation of **k**-vector conservation allowing observation of the scattering from entire branches of the acoustic and optical phonons [12]. At the same time, the fraction of the surface to interior atoms increases in smaller particles leading to further modification of the phonon density of states [12,13]. Confinement of the electronic states strongly affect the electron-phonon interaction, which should be also taken into account for analysis of the Raman spectra [14,15].

The phonon states of *isolated* Si nanoparticles have been relatively unexplored experimentally -- publications on *in situ* measurements of nc-Si are rare [16]. Previous Raman studies have generally focused on samples with Si particles within a matrix or with ligands [2,4,5,17,18]. In these systems, the influence of a matrix or surface contamination on the phonon spectra cannot be neglected. Thus, in the analysis of the observed shifts and broadening of the optical phonon lines, it was difficult to distinguish between effects due to phonon confinement, surface state modification, and matrix-induced stress.

In this paper, we report on *in situ* Raman studies of ultra-small Si particles grown in ultrahigh vacuum. We have studied the phonon states of the Si nanoparticles free of chemisorbed species as well as changes in the phonon states induced by the crystallization process. The main experimental problem was a weak signal from the system with extremely small scattering volume. The situation has been drastically improved by using interference enhanced Raman scattering (IERS) [19] combined with the multichannel detection [20]. Raman signal from the ultrathin films was enhanced by a factor of 15-20 due to the bilayer structure, which makes IERS sensitive even to submonolayer coverage. Recently this technique provided useful information about the vibrations of surface and near-surface atoms of carbon nanocrystallite clusters and ultrathin films [13] and isolated Ge nanoparticles [21].

Reflection electron energy loss spectroscopy (EELS) involves the scattering of a monochromatic beam of low energy electrons from a sample and analyzing the energy distribution in the reflected beam. For losses arising from the dipole scattering mechanism, the observed spectrum is related to the dielectric function of the material. EELS has been shown to be a valuable tool in the measure of surface optical constants [22] and the study of the absorption edge and subgap absorption in thin films of amorphous semiconductors [23] and isolated nanoparticles [24]. In this paper, we report preliminary *in situ* EELS measurements of the optical gap of Si nanoparticles.

EXPERIMENT

Ultrathin layers of Si were grown on amorphous MgO or Ag buffer layers at room temperature by dc magnetron sputtering in an ultrahigh vacuum (UHV) chamber. A power of 6 W/cm^2 was applied to the Si sputter target. The background pressure of Ar was kept around 4 mTorr during the Si growth process. Before deposition of Si, the substrates were annealed at 500˚C. The growth rate of Si, calibrated by both *ex situ* elipsometry and profilometry, was about 0.5 Å/sec. The average thickness of the Si layers d ranged from monolayer coverage up to 200 Å. In the following, the Si samples will be identified by their value of d. To crystallize the Si ultrathin layers, the samples were heated up to about 500ºC by electron emission and thermoradiation. The temperature of the sample was estimated by means of both a thermocouple attached to the sample holder and a pyrometer.

Silicon forms nanometer-size clusters of a hemispherical shape on the substrate. The average size and concentration of the Si clusters varied with d. For example, in a d = 30 Å film on Ag, the Si clusters had a 20 – 50 Å base width and were 15 – 30 Å high, as measured by high resolution electron microscopy. Our preliminary results with *in situ* core-level x-ray photoemission (XPS) show that at $d \leq 50$ Å, Si forms nanoscale islands on MgO substrates. For thicker layers of Si, the characteristic MgO signal in the XPS spectra quickly disappears, corresponding to a complete coverage of the buffer-layer surface with Si atoms. It is similar to the growth regime of Ge nanoparticles investigated previously with the same apparatus [21]. It was shown that the Ge clusters have a hemispherical shape and each of them contains about (10 – 20)d [Å] atoms. Electron microscopy confirms that this relation can be also used in our case for estimating the Si particle size.

The Raman measurements were performed *in situ* at room temperature and at a pressure of 2 x 10^{-10} torr in the UHV system. Interference enhancement of the laser electric field close to the surface (the position of the Si nanoparticles) was achieved by utilizing a bilayer structure, which consists of a transparent dielectric film (MgO) deposited on a metallic layer (Ag) [19,25]. The entire structure was grown on a Si

substrate. The thickness of the amorphous Ag, which works in the bilayer structure as a light reflector, was about 2000 Å. This is thick enough to completely screen any possible Raman signal from the Si substrate. The 5145 Å line (2.4 eV) of an Ar^+-ion laser was used for excitation of the Raman spectra. The MgO layer was grown with a thickness of 500 Å, as calculated to give optimal interference enhancement at the exciting wavelength. The choice for the dielectric buffer layer (MgO) was determined by the two following reasons. First, the Raman signal of MgO is weak at the green light excitation and, second, the analysis of the photoemission spectra is easier than, e.g. in case of a SiO_2 buffer, which also contains Si atoms.

Raman spectra were measured with a SPEX Triplemate spectrometer equipped with a charge-coupled device (CCD) detector cooled with liquid nitrogen. The resolution was about 1.5 cm^{-1}. The intensity of the Raman signal was analyzed in the conventional backscattering configuration with the laser beam and scattered light perpendicular to the plane of the sample.

Electron energy loss spectra were measured with an LK2000 HREELS spectrometer with a rotatable analyzer operated with 5 eV pass energies yielding a resolution of approximately 30 meV. Ultrathin Si was deposited on SiO_2 buffer layers (prepared by dc magnetron sputtering, about 240 Å thick) on Si substrates. Incident electrons were at an energy of 50 eV.

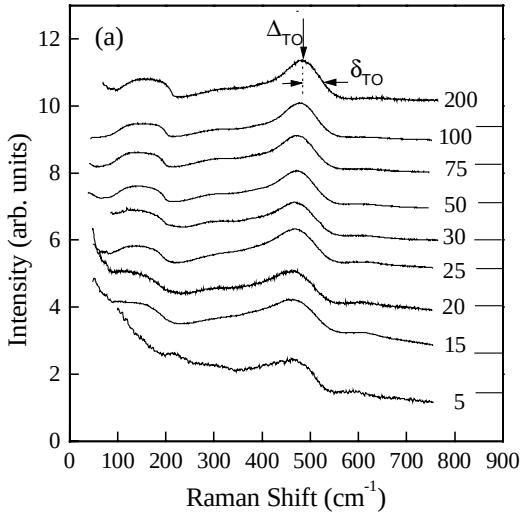

Figure 1. Normalized Raman spectra of amorphous Si layers measured with excitation at 2.4 eV. The respective average thicknesses are given next to the spectra in Å. The spectra were vertically shifted for clarity. The horizontal solid lines indicate the zero-signal levels.

RESULTS AND DISCUSSION

Raman spectra for samples with a different average thickness of the Si layer grown on MgO are shown in Fig. 1. They are similar to that of amorphous Si (a-Si) and consist of the TA, 2TA and TO strong bands centered around 150, 300, and 480 cm^{-1}, respectively, and the weak LA shoulder at 370 cm^{-1} [26-28]. As the film thickness decreases, the high frequency half width at half maximum (HWHM) of the TO band, δ_{TO} defined as shown in Fig. 1, changes from 35 to 50 cm^{-1}. At the same time the position of the maximum Δ_{TO} moves towards the low Raman shifts. The dependencies of Δ_{TO} and δ_{TO} on *d* are presented in Fig. 2. Similar features of the phonon spectra were reported for a-Si thick films grown at different conditions and, e.g., it has been shown Δ_{TO} reflects the distribution of the *sp*-bonds in a-Si [12].

We explain the broadening of our spectra by the modification of the phonon density of states due to changes in the

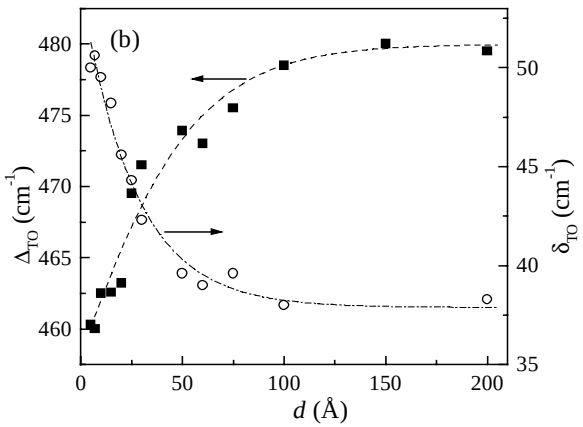

Figure 2. The HWHM δ_{TO} and the position Δ_{TO} of the TO Raman peak as functions of the average thickness of the Si layers. Dashed lines guide the eye.

angular distribution of the *sp*-bonds in the near-surface atomic layers and dangling bonds on the surface. Indeed, in ultra-thin Si films, the fraction of the surface atoms to interior atoms increases making the surface effects more pronounced. Our experiments are important to distinguish between size-dependent modifications of the phonon density of states from that due to contamination of the Si surface with hydrogen or oxygen. The latter might be neglected for our samples, but could be very strong in, e.g., porous Si. Note that the significant variation in the phonon spectra occurs for the samples with $d < 50$ Å. Recall that our preliminary XPS results demonstrate that near this value of d, Si forms nanoscale islands on the substrate.

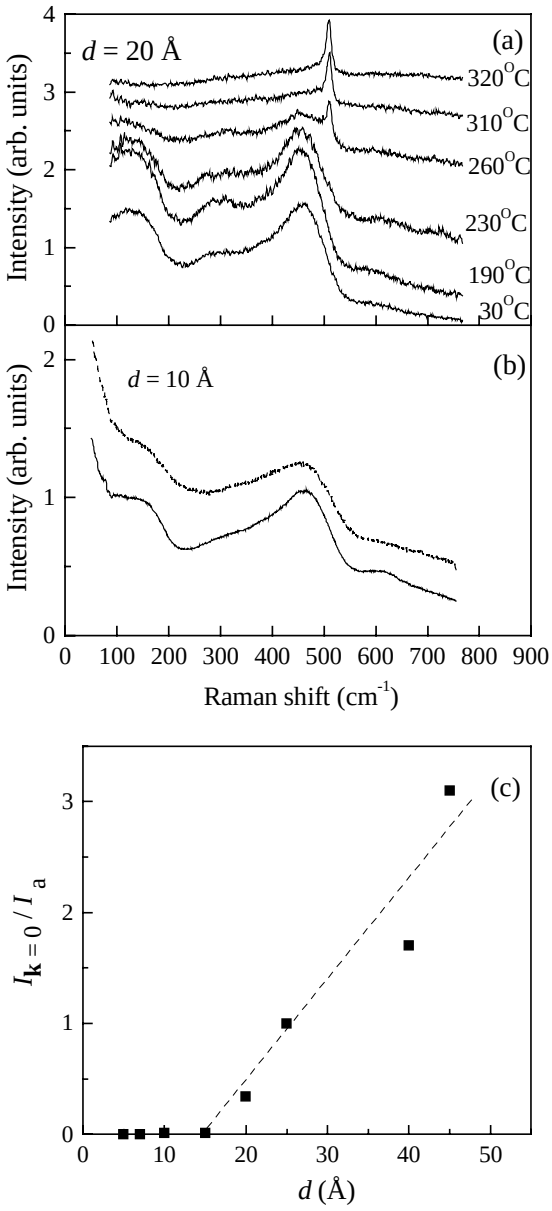

Figure 3. (a) Normalized Raman spectra of the 20 Å sample measured at different temperatures during crystallization process. The spectra were vertically shifted and the constant background was subtracted for clarity. (b) Raman spectra of the 10Å sample before (solid line) and after annealing (dashed line). (c) The ratio of the **k**=0 peak intensity $I_{\mathbf{k}=0}$ to that of the amorphous background I_a as a function of the average thickness of the Si layers. Dashed line guides the eye.

After heating the samples, a remarkable transformation in the Raman spectra was observed. Fig. 3(a) shows several spectra for the 20 Å sample taken at different temperatures. The sharp crystalline peak arises in the Raman spectra when the temperature increases to more than T ≈ 260ºC. At the same time, the intensity of the amorphous-like broad features decreases disappearing at T > 320ºC. This indicates a partial recovering of the **k**-vector conservation condition with crystallization of the Si layers allowing only scattering by optical phonons at the zone center (**k**=0), where the TO and LO phonons in bulk crystalline Si are degenerated [29]. At room temperature, the position of the crystalline peak in our samples is about 519 ± 1 cm^{-1}, which is close to that in bulk [30]. Its full width at half maximum is about 7 cm^{-1}, which is about two times wider than that in Si single crystal. Although one expects a red shift in the position of the optical phonon line in nanoparticles due to confinement, no strong systematic shift of this peak was observed with our experimental accuracy (1.5 cm^{-1}). In our system, it can be explained by the partial compensation of the confinement effect by compressive strain, which works in the opposite direction. High-resolution Raman measurements are required for detailed studies of these effects in

nc-Si. However, these experiments would be limited by the extremely small scattering volume of Si nanoparticles

As the average thickness of the Si layer decreases, the relative intensity of the **k**=0 peak to the intensity of the amorphous-like broad peak at 480 cm^{-1} decreases and the **k**=0 peak disappears for Si films with $d \leq 10$ Å. The ratio of the **k**=0 peak intensity to the amorphous-like background intensity is shown in Fig.3(c). In the case of the relatively thick films, with *d* greater than 50 Å, the complete **k**-vector conservation could be achieved after annealing, which manifests itself by the disappearance of the amorphous-like features in the Raman spectra. For Si films with d less than 10 Å, the Raman spectra do not change with annealing and practically no modifications have been observed even after heating up to 500ºC. Two corresponding spectra of the 10 Å sample grown on a Ag buffer layer and measured at room temperature before and after annealing are shown in Fig. 3(b).

This result is important for the determination of the minimum size of a crystalline system, which can satisfy **k**-vector conservation conditions. According to our estimations, the transition between crystalline- and amorphous-like behavior takes place in the samples with an average number of Si atoms in one hemispherical particle equal to about three hundred. The role of surface and near-surface layers requires additional theoretical studies. The comparative study of the Raman scattering spectra and the high resolution electron microscopy images will be published elsewhere [31].

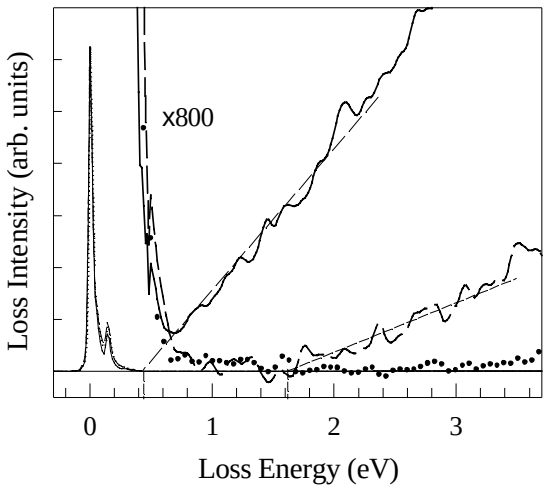

Figure 4. EELS spectra for SiO_2 substrate (dotted) and ultrathin (*d*=5Å) Si: as-deposited (solid) and annealed (dashed). Light dashed lines guide the eye to the onset of electronic transitions.

Electron energy loss spectra for a sample with an average thickness d = 5 Å of Si grown on SiO_2 are shown in Fig. 4. The three spectra were normalized to the elastic peak intensity. An intense peak at 145 meV, appearing in all three spectra, is due to a dipole-active phonon in the SiO_2 substrate [24]. On the same plot, the lower intensity electronic transitions are shown with magnification to illustrate the onset of electronic transitions in the SiO_2 substrate, the as-deposited Si layer, and the annealed (T > 260ºC) Si layer. The SiO_2 substrate has no transitions evident below 3.8 eV. The onset of electronic states in the pristine sample occurs at lower energy than that seen in the annealed sample. Qualitatively, it can be estimated that the onset of electronic transitions is at about 0.4 eV and 1.6 eV before and after annealing, respectively. A similar, quantitative result can be extracted from the EELS data by computing the absorption coefficient $\alpha(\omega)$ [23] and using analogous techniques as those employed to estimate the optical gap in amorphous semiconductors [32]. We have thus demonstrated the ability to measure optical gap differences in nanoparticles of silicon.

CONCLUSIONS

In conclusion, we studied the phonon states of Si nanoparticles grown and measured in ultrahigh vacuum. Marked transformation in the phonon density of states

and the relaxation of the **k**-vector conservation condition with decrease in size of the Si nanoparticles were detected.

ACKNOWLEDGMENTS

The authors are grateful to S. Rouvimov for high resolution electron microscopy measurements and to V. I. Merkulov for useful discussions.

This work was supported by USDOE Grant DE-FG02-84ER45095 and NSF Grant DMR-96-23315.

REFERENCES

1. A. G. Cullis and L. T. Canham, Nature **353** (6342), 335 (1991).
2. A. G. Cullis, L. T. Canham, and P. D. J. Calcott, J. Appl. Phys. **82** (3), 909 (1997).
3. K. Eberl, K. Brunner, and W. Winter, Thin Solid Films **294** (1), 98 (1997).
4. E. W. Forsythe, E. A. Whittaker, F. H. Pollak *et al*., in *Microcrystalline and Nanocrystalline Semiconductors*, edited by R. W. Collins (MRS, Pittsburgh, 1994), Vol. 358.
5. X. S. Zhao, Y. R. Ge, J. Schroeder *et al*., Appl. Phys. Lett. **65** (16), 2033 (1994).
6. W. L. Wilson, P. F. Szajowski, and L. E. Brus, Science **262** (5137), 1242 (1993).
7. S. Schuppler, Y. J. Chabal, F. M. Ross *et al*., Phys. Rev. Lett. **72** (16), 2648 (1994).
8. D. Kovalev, H. Heckler, B. Averboukh *et al*., Phys. Rev. Lett. , accepted for publication (1998).
9. R. Alben, D. Weaire, Jr. J. E. Smith *et al*., Phys. Rev. B **11**, 2271 (1975).
10. T. Takagahara, J. Lumin. **70** (1), 129 (1996).
11. A. Ekimov, J. Lumin. **70** (1), 1 (1996).
12. J.S. Lannin, "Raman Scattering of Amorphous Si, Ge, and their Alloys," in *Semiconductors and Semimetals*, edited by J. I. Pankove, v. 21B (Academic Press, Orlando, 1984), p. 159.
13. J.S. Lannin, V.I. Merkulov, and J.M. Cowley, in *Advances in Microcrystalline and Nanocrystalline Semiconductors : Materials Research Society Symposia Proceedings No. 452*, edited by R. W. Collins, *et al*., (MRS, Pittsburgh, 1996), p. 225.
14. C. Trallero-Giner, A. Debernardi, M. Cardona *et al*., Phys. Rev. B **57** (8), 4664 (1998).
15. A. A. Sirenko, V. I. Belitsky, T. Ruf *et al*., Phys. Rev. B **58** (4), 2077 (1998).
16. S. Hayashi and H. Abe, Jpn. J. Appl. Phys. **23**, L824 (1984).
17. Z. Igbal, S. Veprek, A.P. Webb *et al*., Solid State Comm. **37**, 993 (1981).
18. Y. Gao and T. López-Ríos, Solid State Commun. **60**, 55 (1986).
19. G.A.N. Connel, R. J. Nemanich, and C.C. Tsai, Appl. Phys. Lett. **36**, 31 (1980).
20. J.C. Tsang, in *Light Scattering in Solids*, edited by M. Cardona and G. Güntherodt, Topics in Applied Physics, v. V (Springer-Verlag, Berlin, 1989), p. 233.
21. J. Fortner and J. S. Lannin, Surf. Sci. **254** (1), 251 (1991).
22. H. Froitzheim, H. Ibach, and D.L. Mills, Phys. Rev. B. **11** (12), 4980 (1975).
23. G.P. Lopinski and J.S. Lannin, Appl. Phys. Lett. **69** (16), 2400 (1996).
24. Gregory P. Lopinski, Vladimir I. Merkulov, and Jeffrey S. Lannin, Phys. Rev. Lett. **80** (19), 4241 (1998).
25. W. S. Bacsa and J. S. Lannin, Appl. Phys. Lett. **61** (1), 19 (1992).
26. J. E. Smith, M. H. Brodsky, B. L. Crowder *et al*., Phys. Rev. Lett. **26**, 642 (1971).
27. J.S. Lannin and P.J. Carrol, Philos. Mag. **45**, 155 (1982).
28. G. Nilsen and G. Nelin, Phys. Rev. B **6**, 3777 (1972).
29. Peter Y. Yu and Manuel Cardona, *Fundamentals of Semiconductors: Physics and Materials Properties* (Springer-Verlag, Berlin, 1995) , p 103.
30. D. Bimberg, *et al.*, in *Numerical Data and Functional Relationships in Science and Technology*, edited by O. Madelung, Landolt-Börnstein, New Series, Group III, v. 17a (Springer, Berlin, 1982), p. 72.
31. A. Sirenko, J.R. Fox, S. Rouvimov *et al*., "To be published."
32. G.D. Cody, "The Optical Absorption Edge of a-Si:H," in *Semiconductors and Semimetals*, edited by J. I. Pankove, v. 21B (Academic Press, Orlando, 1984), p. 11.